Nanoscale

Accepted Manuscript

This article can be cited before page numbers have been issued, to do this please use: X. Zhu, J. huang, J. Liu, H. Zhang, J. Jiang and R. Yu, *Nanoscale*, 2017, DOI: 10.1039/C7NR00958E.

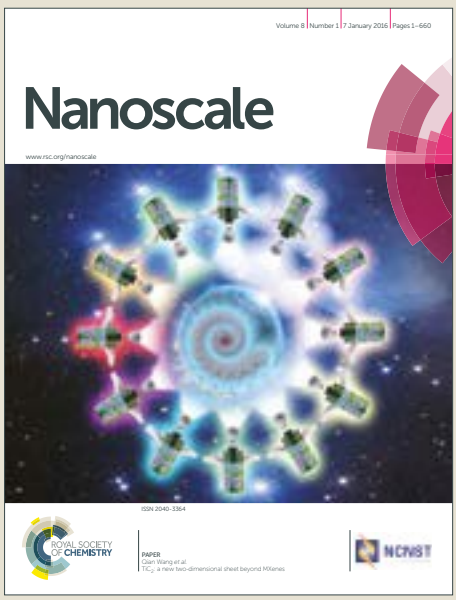

View Article Online
DOI: 10.1039/C7NR00958E

Journal Name

ARTICLE

Dual enzyme-inorganic hybrid nanoflowers incorporated microfluidic paper-based analytic devices (μPADs) biosensor for sensitive visualized detection of glucose

Received 00th January 20xx,

Accepted 00th January 20xx

DOI: 10.1039/x0xx00000x

www.rsc.org/

Xueli Zhu, Jin Huang, Jinwen Liu, Hang Zhang, Jianhui Jiang*, Ruqin Yu*

A novel microfluidic paper-based analytic devices (μPADs) biosensor is developed for sensitive and visualized detection of glucose. This biosensor is easily fabricated using the wax printing technique, with a hybrid nanocomplex composed of dual enzymes of glucose oxidase (GOx) and horseradish peroxidase (HRP) and $Cu_3(PO_4)_2$ inorganic nanocrystals incorporated in the detection zones. The hybrid nanocomplex is found to exhibit a flower-like structure, which allows co-immobilization of these two enzymes in a biocompatible environment. These nanoflowers not only preserve the activity and enhance the stability for the enzymes, but also facilitate transport of the substrates between the two enzymes. The biosensor is demonstrated to enable rapid and sensitive quantification of glucose in the concentration range of 0.1 - 10 mM with a limit of detection (LOD) of 25 μM. It is also shown to be applicable to colorimetric quantitative detection of glucose in human serum and whole blood samples, implying its potential for clinical applications.

Introduction

Enzymes, as biological species with excellent catalytic activity and reaction specificity, have been widely used in the fields like chemistry, medicine, pharmaceutical science, agriculture and industry.[1-5] The emergence of excitingly enzyme-mimetic nanomaterials that possess an intrinsic peroxidase like activity, including magnetic nanoparticles (MNPs), metal and its oxide nanomaterials, carbon nanomaterials *etc*,[6-14] created new opportunities for the application of nanomaterials in these fileds. Additionally, this kind of "nanozyme" is more inexpensive, stable, durable and easier to store compared with biological enzymes.[15-19] Nevertheless, nanozymes suffer from their own drawbacks, for instance, some of them possess toxicity, poor biocompatibility, harsh working condition, complicated procedure of preparation and relatively low catalytic activity, which restrict their widespread applications.

The development and application of biomolecule-metal phosphate have attracted considerable interest in potential applications related to proteomic analysis, sensing, drug delivery, catalysis, tissue engineering and so on,[20-29] since the report of a novel synthetic strategy for protein-inorganic hybrid nanoflowers.[30] The previous results show that these nanoflowers are non-toxic, easy to prepare, highly biocompatible. They also exhibit dramatically enhanced activity, stability, durability and reusability due to the immobilization of enzymes in the nanoflowers and their high specific surface compared with free enzyme and most enzyme-mimetic nanomatarials.[31-33] Given their many advantages, these nanoflowers open the avenues for explore new methodologies for biosensor and biomedical applications.

Microfluidic paper-based analytic devices (μPADs), since firstly developed,[34] has drawn increasing attention as a powerful tool for rapid qualitative and quantitative analysis in fields such as biochemical analysis, food safety, environmental monitoring, and point-of-care clinical diagnostics, by integration with different detection techniques including chemilunescence, mass spectrometry, colorimetric and electrochemical.[35-40] As a widely applicable method, μPADs possess variety of advantages such as simplicity, low cost, visual detection, high throughput, portability and minimal sample consumption, making them ideal for analytical practices with limited resources. Furthermore, as the major component of μPADs, white paper can provide high contrast with a colored indicator, allowing colorimetric assays to be specially useful for qualitative and quantitatively analyse of a range of analytes.

Here we develop a novel paper-based biosensor for directly quantitative detection of glucose using wax printing μPADs with deposited enzyme-inorganic hybrid nanoflowers. Glucose level in blood is related to diabetes mellitus, one of the most common diseases globally, and it is of great importance for rapid and reliable detection of glucose for diagnosis and

State Key Laboratory for Chemo/Biosensing and Chemometrics, College of Chemistry and Chemical Engineering, Hunan University, Changsha, 410082, P. R. China. el.: 86-731-8822577; fax: 86-731-8822782; E-mail addresses: jianhuijiang@hnu.edu.cn (J.-H. Jiang), rqyu@hnu.edu.cn (R.-Q. Yu).
Electronic Supplementary Information (ESI) available: [details of any supplementary information available should be included here]. See DOI: 10.1039/x0xx00000x

View Article Online
DOI: 10.1039/C7NR00958E

monitoring of diabetes. Many of current methods for glucose detection suffer from the drawbacks such as high cost, time-consuming, complicated operations, sophisticated instrumentation, undesirable detection limit or incapability of using for whole blood samples.[10-11, 41-45] A convenient yet effective approach for monitoring glucose levels is still urgently needed. Our developed biosensor for glucose relies on the combination of μPADs and enzyme-inorganic hybrid nanoflowers, as illustrated in Scheme 1. A hybrid nanoflower complex of two enzymes, glucose oxidase (GOx) and horseradish peroxidase, with $Cu_3(PO_4)_2$ nanocrystal is synthesized through a self-assembly process. The nanocomplex allows co-immobilization of two enzymes in a biocompatible nanostructure, which not only preserves the activity and enhances the stability for the enzymes, but also facilitates mass transfer of the substrates between and to the enzymes. A μPAD is design and fabricated using the standard wax printing technique, which consists of eight circular detection zones, microfluidic channels, and one central zone for sample injection. The biosensor is then readily prepared by depositing the hybrid nanoflowers on the detection zones in the designed μPAD. When a sample introduced in the central zone, the glucose-containing solution can be spontaneously distributed through the microfluidic channels. At the detection zones, glucose is used by GOx to produce H_2O_2, which in turn be used by HRP to oxidize a colorless substrate TMB into a blue product, enabling colorimetric detection of glucose in the sample. Because the high activity of the enzymes in the hybrid nanoflowers and the simplicity of the fabridication and operation of the μPADs, the developed biosensor can provide a simple, portable, low-cost platform for highly sensitive detection of glucose. Moreover, because the paper-based microfluidic channel can filter the cells and only the glucose solution can be distributed to the detection zone, which eliminates the interference from red cells with the colorimetric detection of glucose, our sensor hold the potential for direct assay of glucose even in complicated whole blood samples.

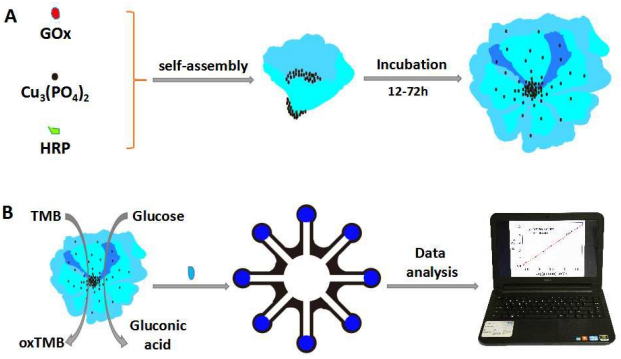

Scheme. 1 Illustration of (A) the formation process of nanoflowers, and (B) the biosensing strategy for the detection of glucose based on the integration of nanoflowers and μPADs.

Experimental

Chemicals and materials

GOx and HRP were obtained from Merck Millipore (USA). Glucose, fructose, mannose, galactose, BSA were all purchased from Sigma Aldrich (USA). DNA was synthesized by Shanghai Sangon Biotechnology Co. Ltd. (Shanghai, China). $MgCl_2{\cdot}6H_2O$, $Cu_2SO_4{\cdot}5H_2O$, $CaCl_2{\cdot}6H_2O$, NaCl, KCl were aquired from Sinopharm Chemical Reagent Co. Ltd. (Shanghai, China). Whatman grade 1 chromatography filter paper was obtained from GE Healthcare (UK). Human serum samples was provided by Xiangya Hospital at Central South Unversity. Other regents used in the work were of analytical grade and used as received. All stock solutions were prepared with ultrapure water (resistance>18.2) obtained from a milli-Q water purification system (Billerica, MA). All experiments were performed at room temperature unless specific mention was made otherwise.

Design and fabrication of the μPAD

The μPADs were produced by the wax patterning fabrication process.[46] The wax patterns were designed using CorelDraw X7 software, followed by printing wax on chromatography filter paper by a wax printer (Xerox Colorqube 8570). The printed paper was heat treated at 150 °C for 2 min and then cooled to room temperature so that the wax can melt and penetrate through the paper to form hydrophobic wax barriers. As shown in Scheme 1, the μPAD consists of eight circular detection zones (5 mm), microfluidic channels (3 mm width and 10mm length), and one central zone (15 mm) for sample injection.

Preparation of the GOx&HRP-$Cu_3(PO_4)_2$ hybrid nanoflowers

The synthesis of GOx&HRP-$Cu_3(PO_4)_2$ nanoflowers was performed according to a literature method.[30] Briefly, 20 μL of aqueous $CuSO_4$ solution (20 mM) was added in 480 μL of phosphate buffered saline (PBS) solution (pH 7.4) containing different concentrations of GOx and HRP. The reaction was allowed to proceed at room temperature for 12 to 72 h, in which the suspension of the as-prepared hybrid nanoflowers were obtained.

Measurements and characterizations

For SEM analysis, the suspension of the as-prepared nanoflowers was centrifugated and washed three times, and then dropped on a silicon wafer. The size and the morphology of the nanoflowers were characterized using a field-emission scanning electron microscope (SEM) (Sigma HD, Carl Zeiss) with an accelerating voltage of 10 kV. The crystalline structures of the as-prepared samples were obtained from an X-ray diffractometer (Bruker, Germany) using Cu Kα radiation (λ= 0.15405 nm). UV-vis absorption spectra were recorded on a UV-2450 spectrometer.

Preparation of the μPAD biosensor and colorimetric detection

For the fabrication of the biosensor for glucose, 0.4 μL TMB (50 mM) and 1 μL suspension of the as-prepared GOx&HRP-$Cu_3(PO_4)_2$ hybrid nanoflowers were mixed and added on the

View Article Online
DOI: 10.1039/C7NR00958E

detection zones of the device. The device was dried at room temperature for 15 min in a humidified atmosphere. The obtained biosensor can be stored at 4 °C in a humidified atmosphere with no substantial loss of sensitivity observed for 2 weeks.

For the detection of glucose in the samples, a 65 µL of samples with different concentrations of glucose were dropped in the central zone, from which the solution was spontaneously distributed to the detection zones through the microfluidic channels. After 10 min reaction, the colorimetric signals obtained at the detection zones were recorded using a Nikon digital camera. The photos were converted to gray scale, which was used to analyze the color intensity and gradient by ImageJ software.

The proposed µPADs with hybrid nanoflowers were investigated in human whole blood samples. The samples were collected at Xiangya Hospital (Changsha, China) from 8 patients using borosilicate glass microcapillary tubes. All samples were stored at -20 °C and thawed at ambient temperature before use. The procedure of detection was the same as described above.

Results and discussion

Synthesis and characterization of GOx&HRP-$Cu_3(PO_4)_2$ nanoflowers

It was reported that biomolecule-metal phosphate based protein-inorganic hybrid nanocomplex provided a biocompatible platform to immobilize enzymes with high catalytic activity and enhanced stability.[30] Motivated by these findings, we chose to synthesize the GOx&HRP-$Cu_3(PO_4)_2$ based hybrid nanostructure. The nanostructure was synthesized readily by adding $CuSO_4$ solution in PBS (pH 7.4) containing GOx and HRP. The nanocomplex was obtained as blue precipitates after 12 to 72 h reaction. The formation of nanoflowers comprised three steps:[20] (a) nucleation and the formation of primary copper phosphate crystals, (b) Agglomerates formation of enzymes and Cu^{2+} through binding with amide groups in the enzyme backbone, and (c) the complete formation of nanoflowers.

Scanning electron microscope (SEM) was used for characterizing the morphology of the nanocomplex, as shown in Figure 1. With the concentration of GOx over 0.01 mg·mL^{-1} (0.01, 0.05, 0.1, 0.5 mg·mL^{-1}), hybrid nanocomplexes with structures like flowers were obtained. Interestingly, the size of these nanoflower structures became smaller with increasing enzyme concentrations (Fig. S1 in ESI†). This result indicated that the number of nucleation sites increased with the increasing concentration of GOx, revealing that the enzyme molecules facilitated the nucleation process. Presumably, the amino groups on the protein surface might coordinate with Cu^{2+} and result in a higher local Cu^{2+} concentration, mediating the nucleation process. A control experiment with no enzyme showed that the nanoflowers were not obtained in the absence of enzyme, which confirmed the essential role for the protein in nucleation. In addition, in the presence of 0.5 mg·mL^{-1} GOx, when HRP of different concentrations (0.01, 0.1, 0.5 mg·mL^{-1}) were added in the solution, we obtained nanoflowers with similar size about 20 µm (Fig. S2 in the ESI†). This result implied the co-existence of HRP with GOx did not affect the formation of the nanoflowers, suggesting the possibility of co-immobilization of two enzymes in the nanoflowers. Further evidence from analysis of different incubation times (2, 12, 36, 72 h) revealed that the nanoflowers continued to grow with increasing reaction time, exhibiting different morphologies at varying reaction time and forming compact flower-like nanostructures after 36 h reaction (Fig. S3 in ESI†).

The X-ray powder diffraction (XRD) patterns (Fig. S4 in ESI†) revealed the crystallographic structures of the nanostructures obtained with and without of enzymes. The diffraction spectra showed typical peaks of $Cu_3(PO_4)_2$ (JPSCD 00-022-0548), implying the major crystalline components for the nanostructures were $Cu_3(PO_4)_2$. The energy dispersive X-ray spectroscopy (EDX) analysis (Fig. S5 in ESI†) confirmed that the nanoflowers were mainly composed of the elements of P, Cu, C, and O, giving evidence for the $Cu_3(PO_4)_2$ component in the nanoflowers.

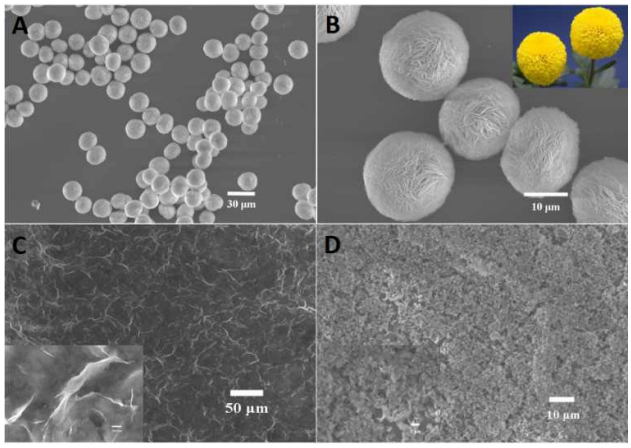

Fig. 1. (A and B) SEM images of GOx&HRP-$Cu_3(PO_4)_2$ nanoflowers. Inset: real flowers in nature; (C) In the absence of $CuSO_4$; (D) In the absence of GOx and HRP.

Glucose detection using the nanoflower-based µPADs biosensor

To demonstrate the advantage of the GOx&HRP-$Cu_3(PO_4)_2$ nanoflowers based biosensor for glucose detection, we investigated its performance against a µPAD biosensor prepared using mixtures of free enzymes or the HRP-$Cu_3(PO_4)_2$ and GOx-$Cu_3(PO_4)_2$ nanoflowers. Samples with glucose of different concentrations were added directly in the detection zones with immobilized nano-enzyme and free enzyme of the same concentration (0.5 mg·mL^{-1} GOx, 0.1 mg·mL^{-1} HRP). As shown in Figure 2A, it is clear that the detection zones with the immobilized GOx&HRP-$Cu_3(PO_4)_2$ nanoflowers show much darker blue color than those with free enzymes, indicating that the hybrid nanoflowers creates a useful platform to preserve

View Article Online
DOI: 10.1039/C7NR00958E

and enhance the activity of the enzymes and thus afford improved sensitivity. Interestingly, the GOx&HRP-$Cu_3(PO_4)_2$ based sensor also displayed darker blue color than the sensor based on the mixture of the GOx-$Cu_3(PO_4)_2$ nanoflowers and the HRP-$Cu_3(PO_4)_2$,nanoflowers, suggesting that the GOx&HRP-$Cu_3(PO_4)_2$ nanoflower even had higher activity than the mixture. Presumably, the enhanced activity of enzymes in the GOx&HRP-$Cu_3(PO_4)_2$ nanoflowers was attributed to the large specific surface and the very short-distance transport of the substrates between two enzymes in coherence with the enzymatic cascade reactions.[47] Another control experiment using the sensor based on the GOx-$Cu_3(PO_4)_2$ nanoflowers revealed that the nanoflowers did not have substantial peroxidase-like activity, and no appreciable color changed was obtained in this μPAD. A further investigation was performed by mixing the solutions for the nanoflowers or enzymes with TMB and glucose also showed that the GOx&HRP-$Cu_3(PO_4)_2$ nanoflowers gave the maximum absorbance response (Figure 2B), confirming the enhancement of enzymatic activity in the nanoflowers.

To investigate the effect of morphologies for the GOx&HRP-$Cu_3(PO_4)_2$ nanoflowers on the sensor's response, the nanoflowers obtained after 12 h and 36 h, respectively, reactions were used for detection of glucose (Fig. S6 in ESI†). It was found that the nanoflowers obtained after 12 h reaction showed much higher activity. According to previous SEM observations, the nanoflowers obtained after 12 h reaction had a less compact and more porous structure than those obtained after 36 h reaction. This porous structure increased largely the surface area and improved the mass transfer rate, thus affording better catalytic activity in the detection.

In order to achieve the quantitative detection of glucose using the developed biosensor, different concentrations of glucose (0.1-10 mM) were dropped on the detection zones of the μPADs, and a Nikon digital camera was used to take pictures of the μPAD after 10 min. Photos were converted to gray scale (Fig. S7 in the ESI†), and then analyzed to obtain the color intensities and gradients using ImageJ software. As displayed in Fig. 3, the color of the detection zones gradually changed from colorless to dark blue, and a good linearity between the color intensity and glucose concentration was obtained in the range of 0.1-10 mM (R^2 = 0.9951). The limit of detection (LOD) was 25 μM, which is comparable or lower than those for most existing sensors (Table S1 in the ESI†). In

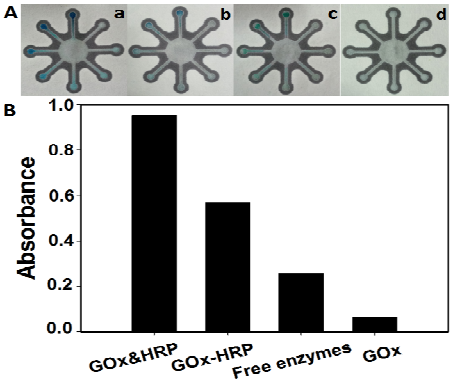

Fig. 2. (A) Color changes responses to 0, 0.1, 0.25, 0.5, 1, 2, 4, 8 mM glucose obtained with μPADs sensor prepared using (a) GOx&HRP-$Cu_3(PO_4)_2$ nanoflowers, (b) mixture of HRP-$Cu_3(PO_4)_2$ and GOx-$Cu_3(PO_4)_2$ nanoflowers, (c) free enzymes, (d) GOx-$Cu_3(PO_4)_2$ nanoflowers. (B) Absorbance readings obtained using the corresponding enzymes or nanoflowers in response to 40 μM glucose.

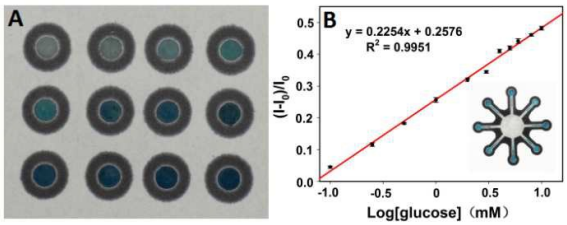

Fig. 3. (A) Photograph of μPADs used for the detection of glucose with concentrations of 0, 0.1, 0.25, 0.5, 1, 2, 3, 4, 5, 6, 8, 10 mM; (B) The linearity of relative color intensity with respect to glucose concentration.

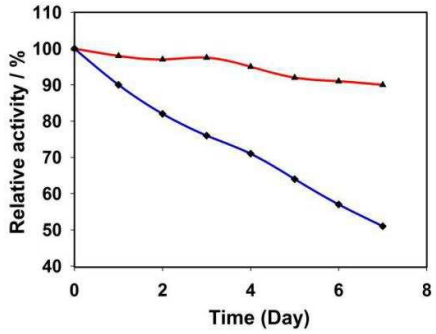

Fig. 4. Storage stability of GOx&HRP-$Cu_3(PO_4)_2$ nanoflowers (red curve) and free enzymes (blue curve) in PBS (pH 7.4) at room temperature.

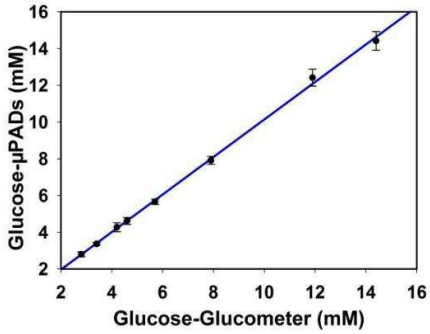

Fig. 5. Determination of the glucose levels in whole blood samples. The detection of glucose in the whole blood with concentrations of 2.8, 3.4, 4.2, 4.6, 5.7, 7.9, 11.9, 14.4 mM.

View Article Online
DOI: 10.1039/C7NR00958E

addition, we found that the long-term stability of the hybrid nanoflowers based sensor was much better than that for the free enzyme based sensor (Fig. 4). Such enhanced stability was attribute to the confined configuration of the immobilized enzymes on $Cu_3(PO_4)_2$ nanocrystals, which could prevent the proteins from denaturation.[48-49]

Performance of the nanoflower-based μPADs for glucose detection in the whole blood

Next, the nanoflower-based μPADs sensor was used to detect the glucose levels in human serum samples collected from patients, some samples were diluted to the desired concentrations. The detection zones exhibited obvious color change from colorless to blue followed the addition of the whole blood samples (Fig. S8 in the ESI†). In accordance with the calibration curve, the concentrations of glucose in the whole blood samples were determined as Fig. 5. Thus, the nanoflower-based μPADs are applicable for human whole blood samples.

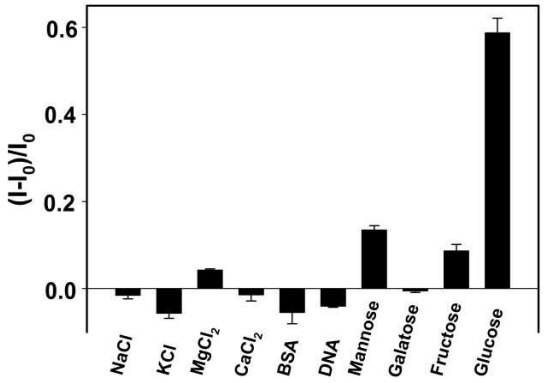

Fig. 6. Response of the method to different analytes at room temperature. The concentration of glucose is 1mM, NaCl, KCl, $MgCl_2$, $CaCl_2$, mannose, galatose, fructose are all 10 mM, BSA and DNA are both 1 $\mu g \cdot L^{-1}$.

Before applying the proposed biosensor for real sample analysis, the selectivity of the nanoflower-based μPAD for glucose was evaluated by monitoring the color intensity change of the detection zone in the presence of various analytes. As displayed in Fig. 6, the relative color intensities of these analytes did not interfere in the detection of glucose, that is to say, the proposed assay shows superior selectivity for glucose detection, which is promising to be applied in real biological samples.

Conclusions

In summary, we have developed a simple, low-cost, colorimetric biosensor for visualized detection of glucose with high sensitivity and stability. The use of dual enzyme-inorganic hybrid nanoflowers in the microfluidic paper-based analytic devices (μPADs) improves the enzymatic activity and stability, and the design of paper-based microfluidic analytic devices (μPADs) affords the very low cost and high contrast for colorimetric and visualized detection. The biosensor is demonstrated to enable rapid and sensitive quantification of glucose in the concentration range of 0.1 - 10 mM with a limit of detection (LOD) of 25 μM. It is also shown to be applicable to colorimetric quantitative detection of glucose in human whole blood samples. In virtue of these advantages, the developed method may have great potential for the low-cost and sensitive monitoring of glucose in real-world clinical point-of-care tests.

Live subject statement

All blood tests described in the project were in agreement with the WHO's rules for "the clinical use of blood". All procedures were performed in compliance with the relevant laws and institutional guidelines. The institutional committee(s) have approved the experiments and that informed consent was obtained for the experimentation with human subjects.

Acknowledgements

This work was supported by NSFC (21527810, 21190041, 21221003).

Ntes and references

1 J. Ye, Y. Chen and Z. Liu, *Angew. Chem. Int. Ed.,* 2014, **53**, 10386-10389.
2 D. S. No, T. Zhao, J. Lee, J. S. Lee and I. H. Kim, *J. Agric. Food Chem.,* 2013, **61**, 231-237.
3 Y. X. Lin, Q. Zhou, Y. P. Lin, D. P. Tang, R. Niesser and D. Knopp, *Anal. Chem.*, 2015, **87**, 8531-8540.
4 X. L. Wu, M. Hou and J. Ge, *Catal. Sci. Technol.*, 2015, **5**, 5077-5085.
5 A. Illanes, A. Cauerhff, L. Wilson and G. R. Castro, *Bioresour. Technol.*, 2012, **115**, 48-57.
6 L. Gao, J. Zhuang, L. Nie, J. Zhang, Y. Zhang, N. Gu, T. Wang, J. Feng, D. Yang, S. Perrett and X. Yan, *Nat. Nanotechnol.*, 2007, **2**, 577-583.
7 J. Pyun, *Angew. Chem. Int. Ed.,* 2011, **50**, 46-48.
8 Y. Song, K. Qu, C. Zhao, J. Ren and X. Qu, *Adv. Mater.*, 2010, **22**, 2206-2210.
9 Y. Ju and J. Kim, *Chem. Commun.*, 2015, **51**, 13752-13755.
10 T. Lin, L. Zhong, J. Wang, L. Guo, H. Wu, Q. Guo, FengFu Fu and G. Chen, *Biosens. Bioelectron.*, 2014, **59**, 89-93.
11 Y. Song, X. Wang, C. Zhao, K. Qu, J. Ren and X. Qu, *Chem. Eur. J.*, 2010, **16**, 3617-3621.
12 Q. Chen, M. Liu, J. Zhao, X. Peng, X. Chen, N. Mi, B. Yin, H. Li, Y. Zhang and S. Yao, *Chem. Commun.*, 2014, **50**, 6771-6774.
13 K. S. Park, M. I. Kim, D. Y. Cho and H. G. Park, *small*, 2011, **7**, 1521-1525.
14 L. Gao, M. Liu, G. Ma, Y. Wang, L. Zhao, Q. Yuan, F. Gao, R. Liu, J. Zhai, Z. Chai, Y. Zhao and X. Gao, *ACS nano*, 2015, **9**, 10979-10990.
15 J. S. Schmid, B. Dordick, A. Hauer, M. Kiener, M. Wubbolts and B. Witholt, *Nature*, 2001, **409**, 258-268.
16 J. Barber, *Chem. Soc. Rev.*, 2009, **38**, 185-196.
17 Y. Zhang, J. Ge, Z. Liu, *ACS Catal.*, 2015, **5**, 4503-4513.

View Article Online
DOI: 10.1039/C7NR00958E

18 Z. Zhou, R. N. K. Taylor, S. Kullmann, H. X. Bao and M. Hartmann, *Adv. Mater.*, 2011, **23**, 2627-2632.
19 R. N. Patel, *Expert Opin Drug Discov.*, 2008, **3**, 187-245.
20 Z. Lin, Y. Xiao, Y. Q. Yin, W. L. Hu, W. Liu and H. H. Yang, *ACS Appl. Mater. Interfaces*, 2014, **6**, 10775-10782.
21 Y. Y. Huang, X. Ran, Y. H. Lin, J. S. Ren, X. G. Qu, *Chem. Commun.*, 2015, **51**, 4386-4389.
22 R. Ye, C. Zhu, Y. Song, Q. Lu, X. Ge, X. Yang, M. Zhu, D. Du, H. Li and Y. Lin, *small*, 2016, **12**, 3094-3100.
23 L. M. Negron, T. L. Díaz, E. O. O. Quiles, D. D. Matos, B. M. Soto and J. M. Rivera, *Langmuir*, 2016, **32**, 2283-2290.
24 L. B. Wang, Y. C. Wang, R. He, A. Zhuang, X. P. Wang, J. Zeng, J. G. Hou, *J. Am. Chem., Soc.*, 2013, **135**, 1272-1275.
25 X. Hu,J. Hu,J. Tian,Z. Ge,G. Zhang,K. Luo and S. Liu, *J. Am. Chem. Soc.*, 2013, **135**, 17617-17629.
26 J. Sun, J. Ge, W. Liu, M. Lan, H. Zhang, P. Wang, Y. Wang and Z. Niu, *Nanoscale*, 2014, **6**, 255-262.
27 Y. Yu, X. Fei, J. Tan, L. Xu, X. Wang and Y. Wang, *Colloids Surf., B*, 2015, **130**, 299-304.
28 B. Zhang, P. Li, H. Zhang, X. Li, L. Tian, H. Wang and X. Chen, *Appl. Surf. Sci.*, 2016, **366**, 328-338.
29 T. Wei, D. Du, M. J. Zhu, Y. Lin and Z. Dai, *ACS Appl. Mater. Interfaces*, 2016, **8**, 6329-6335.
30 J. Ge, J. Lei and R. N. Zare, *nature nano.*, 2012, **7**, 428-432.
31 L. Duan, H. Wang, J. Liu and Y. Zhang, *Biomed. Phys. Eng. Express*, 2015, **1**, 045101.
32 C. Altinkaynak, S. Tavlasoglu, N. Özdemir, I. Ocsoy, *Appl. Surf. Sci.*, 2016, **93-94**, 105-112.
33 M. Li, M. Luo, F. Li, W. Wang, K. Liu, Q. Liu, Y. Wang, Z. Lu and D. Wang, *J. Phys. Chem. C*, 2016, **120**, 17348-17356.
34 A. W. Martinez, S. T. Pillips, M. J. Butte and G. M. Whitesides, *Angew. Chem. Int. Ed.*, 2007, **46**, 1318-1320.
35 T. Tian, X. Wei, S. Jia, R. Zhang, J. Li, Z. Zhu, H. Zhang, Y. Ma, Z. Lin and C. J. Yang, *Biosens. Bioelectron.*, 2016, **77**, 537-542.
36 T. G. Silva, W. R. de Araujo, R. A. A. Muñoz, E. M. Richter, M. H. P. Santana, W. K. T. Coltro and T. R. L. C. Paixão, *Anal. Chem.*, 2016, **88**, 5145-5151.
37 Y. Qin, S. Pan, M. R. Howlader, R. Ghosh, N. X. Hu and M. J. Deen, *Anal. Chem.*, 2016, **88**, 10384-10389.
38 M. Zhao, H. Li, W. Liu, Y. Guo and W. Chu, *Biosens. Bioelectron.*, 2016, **79**, 581-588.
39 B. Gao, H. Liu and Z. Gu, *Anal. Chem.*, 2016, **88**, 5424-5429.
40 P. Rattanarat, W. Dungchai, D. M. Cate, W. Siangproh, J. Volckens, O. Chailapakul and C. S. Henry, *Anal. Chim. Acta*, 2013, **800**, 50-55.
41 M. Ariza-Avidad, A. Salinas-Castillo and L.F. Capitán-Vallvey, *Biosens. Bioelectron.*, 2016, **77**, 51-55.
42 P. T. Garcia, T. M. G. Cardoso, C. D. Garcia, E. Carrilho and W. K. T. Coltro, *RSC Adv.*, 2014, **4**, 37637-37644.
43 E. Noiphung, T. Songjaroen, W. Dungchai, C. S. Henry, O. Chailapakul and W. Laiwattanapaisal, *Anal. Chim. Acta*, 2013, **788**, 39-45.
44 H. J. Chun, Y. M. Park, Y. D. Han, Y. H. Jang and H. C. Yoon, *BioChip J.*, 2014, **8**, 218-226.
45 C. Fischer, A. Fraiwan and S. Choi, *Biosens. Bioelectron.*, 2016, **79**, 193-197.
46 E. Carrilho, A. W. Martinez and G. M. Whitesides, *Anal. Chem.*, 2009, **81**, 7091-7095.
47 Z. Li, Y. Zhang, Y. Su, P. Ouyang, J. Ge and Z. Liu, *Chem. Commun.*, 2014, **50**, 12465-12468.
48 J. Kim and J. W. Grate, *Nano Lett.*, 2003, 3, 1219.
49 M. Yan, J. Ge, Z. Liu and P. Ouyang, *J. Am. Chem. Soc.*, 2006, **128**, 11008-11009.